



# Explosive combustion in a closed channel revisited

Paul Clavin<sup>1</sup>  and Zheng Chen<sup>2</sup> 

<sup>1</sup>Aix Marseille Université, CNRS, Centrale Marseille, IRPHE UMR7342, 13384 Marseille, France

<sup>2</sup>SKLTCS, HEDPS, School of Mechanics and Engineering Science, Peking University, Beijing 100871, PR China

**Corresponding author:** Zheng Chen, [cz@pku.edu.cn](mailto:cz@pku.edu.cn)

(Received 9 October 2025; revised 21 January 2026; accepted 17 February 2026)

---

This work investigates the mechanism of deflagration-to-detonation transition (DDT) in a closed channel filled with a stoichiometric hydrogen–air mixture under knocking-relevant conditions (10 atm, 1100 K). We first revisit the low-Mach-number model for a planar flame propagating towards an inert end-gas, deriving an analytical solution that reveals a finite-time singularity in temperature, which remains physically irrelevant without end-gas reactions. The core analysis demonstrates that the transition is triggered by the breakdown of the low-Mach-number approximation due to weak heat release during the end-gas autoignition induction period. The extreme thermal sensitivity of the induction delay to a small increase in temperature (resulting from both adiabatic compression and autoignition reactions) causes a drastic reduction in the time scale of flame dynamics. This leads to acceleration-induced compression waves which quickly steepen into shocks propagating in a combustible gaseous mixture prompt to detonate. A thermal feedback loop between the self-accelerating flame and the compression waves culminates in the catastrophic breakdown of the laminar flame structure associated with the spontaneous onset of a detonation burning quickly the end-gas in a shorter time than the bulk thermal explosion by autoignition. Supporting numerical simulations, in which the induction chemistry is artificially modified without modifying the chemical kinetics controlling the flame propagation, confirm that the DDT is intrinsically linked to the high thermal sensitivity of the reaction scheme controlling the induction delay in the end-gas.

**Key words:** detonation waves, flames, laminar reacting flows

---

## 1. Introduction

The one-dimensional dynamics of a premixed flame propagating in a closed channel is useful in enlightening the physical mechanisms responsible for knocking that occurs

in internal combustion engines (Kagan & Sivashinsky 2013; Wang, Hu & Reitz 2017). The markedly subsonic propagation of a planar flame in a closed channel with a quasi-uniform pressure growth is known as a layered combustion process investigated theoretically by Zeldovich *et al.* (1985). The numerical simulations of planar flames propagating in a stoichiometric hydrogen–air mixture at elevated temperature and pressure performed by Yu & Chen (2015) have shown that, when the initial temperature and pressure reach 1100 K and 10 atm, respectively, a deflagration-to-detonation transition (DDT) occurs before autoignition of the unburned gas (end-gas). These numerical results are important from both fundamental and applied points of view since they point out an unexplained DDT that could be responsible for the important damage of knocking since the overpressure by reflection of the leading shock on the wall is larger than that by autoignition. Using a thin-flame model associated with a one-step chemical kinetics scheme and considering the low-Mach-number regime from which nonlinear compression waves are excluded, Kagan & Sivashinsky (2013) conducted numerical analysis of one-dimensional flames propagating in a closed channel up to autoignition of the end-gas. The numerical study was recently extended to non-uniform initial conditions by Li *et al.* (2025) (but without autoignition to the best of our understanding).

There are many numerical studies on DDT in closed or open channels/tubes (Ciccarellia & Dorofeev 2008; Liberman *et al.* 2010). However, these studies are not in the context of knocking studied here. Only a few studies have reported multi-dimensional simulations of DDT in a closed tube under knocking-relevant conditions (Wei *et al.* 2019; Morii *et al.* 2021; Yang *et al.* 2024). Similar to the one-dimensional simulation by Yu & Chen (2015), end-gas autoignition and detonation development were also observed at elevated temperatures and pressures in these multi-dimensional simulations.

The objective of the present note is to decipher the mechanism of DDT observed in the simulations of Yu & Chen (2015). Following an analytical solution of the low-Mach-number flow associated with a planar flame propagating in a closed vessel (useful for the following), a theoretical analysis is presented showing that the very small energy released in the end-gas during the induction period is responsible for the breakdown of the low-Mach-number approximation leading to the transition to detonation as soon as the induction delay is more sensitive to the temperature than the laminar flame velocity. To illustrate how the highly sensitive rate of small heat release in the end-gas during the induction period influences drastically the DDT onset, the previous numerical simulations (Yu & Chen 2015) are reconsidered by introducing artificially small modifications into the full kinetic scheme. These modifications concern the induction period without modifying either the laminar flame velocity or the inner structure of the laminar flame. Thus, the decisive role played by the chemical kinetics controlling the induction delay in the DDT onset is confirmed by the numerical results.

## **2. Simplified model of combustion in a closed channel**

For later purposes, it is worth beginning to recall briefly the low-Mach-number limit leading to the dynamics of a thin flame front propagating slowly in a closed vessel and associated with a quasi-homogeneous pressure growth. The asymptotic equations in a multi-dimensional geometry have been derived in the pioneering analyses of Sivashinsky (1974, 1979) who gave also an analytical expression in spherical geometry for the pressure growth in a spherical bomb. The markedly subsonic planar flame propagating in a closed tube is extensively analysed in Zeldovich *et al.* (1985) by a theoretical study based on physical insights. The basic assumptions are the following.

- (i) The combustion is initiated by a thin laminar flame starting at  $t = 0$  from the closed end of the channel at  $x = 0$  and the inner structure of the flame is assumed to be in a stable quasi-steady state. The first assumption is that the flame thickness ( $d_L$ ) is negligible compared with the tube length ( $L$ ), i.e.  $d_L/L \ll 1$ . This is equivalent to assuming that the transit time of a fluid particle across the inner structure of the flame ( $\tau_L \equiv d_L/U_L$ ) is much smaller than the transit time for the flame to cross the whole length of the channel ( $\tau_f \equiv L/U_f$  in the absence of DDT), i.e.  $\tau_L \equiv d_L/U_L \ll \tau_f \equiv L/U_f$ , where  $U_L$  and  $U_f \equiv dX_f/dt$  denote, respectively, the laminar flame velocity and the flame propagation speed in the channel,  $x = X_f(t)$  being the flame position. Assuming  $U_f/U_L = O(1)$ , the time scale  $\tau_f \equiv L/U_f$  is of same order of magnitude as  $\tau_e \equiv L/U_L \approx \tau_f \equiv L/U_f$  so that a quasi-steady-state assumption of the inner structure of the flame during its propagation across the tube  $\tau_L \ll \tau_e$  is equivalent to a thin flame front:

$$d_L \ll L \quad \Leftrightarrow \quad \tau_L \ll \tau_e. \quad (2.1)$$

The laminar flame velocity  $U_L(T_{uf})$  is an increasing function of the temperature of the unburned gas  $T_{uf}$  just ahead of the flame with a thermal sensitivity that is larger than unity:  $(T_{uf}/U_L)dU_L/dT_{uf} > 1$ . An eventual pressure dependence of the laminar flame velocity can be easily included in the function  $U_L(T_{uf})$ , especially if the unburned gas flow is isentropic. Another basic assumption of the low-Mach-number model is that the Mach number of the laminar flame velocity is a small number:

$$\varepsilon \equiv U_{L0}/a_{u0} \ll 1, \quad (2.2)$$

and stays small during the combustion process,  $U_L/a_u = O(\varepsilon)$ ,  $u/a_u = O(\varepsilon)$ ,  $a_u$  and  $u$  denoting, respectively, the sound speed in the unburned gas and the flow speed. The subscript 0 denotes the initial state. In the laminar flame theory, the Mach number  $\varepsilon$  is a transcendently small parameter in the limit of large activation energy  $E$ ,  $b \equiv E/k_B T_b$ ,  $\lim_{b \rightarrow \infty} \varepsilon \propto e^{-b/2}$ ,  $T_b$  being the flame temperature. In a stoichiometric hydrogen–air mixture at ordinary conditions the reduced activation energy  $b$  is about 8 and smaller in a stoichiometric hydrogen–oxygen mixture. According to (2.2), the transit time of the acoustic wave across the tube  $\tau_a \equiv L/a_{u0}$  is shorter than the time scale of the flow  $\tau_e \equiv L/U_{L0}$ . The small parameter (2.2) is precisely the ratio of these two time scales,  $\varepsilon = \tau_a/\tau_e$ . Consider a flame disturbed by compression waves whose length scale is of the same order as the tube length (not much smaller)  $\tau_a \approx L/a$ , so that  $\tau_a/\tau_L = \varepsilon L/d_L$ . Then the flame inner structure is in a quasi-steady state ( $\tau_L \ll \tau_a$ ) if

$$d_L/U_L \ll L/a \quad \Leftrightarrow \quad L/d_L \gg 1/\varepsilon \quad (2.3)$$

that is a more restrictive condition than (2.1).

- (ii) Before an eventual sharp transition, attention is focused on the long time scale  $\tau_e \equiv L/U_{L0}$  of the flame motion so that the small effects of fast acoustic waves, such as the vibratory instability of planar flames analysed by Clavin, Pelcé & He (1990), are ignored in the following. Neglecting acoustics, the pressure  $p(t)$  is uniform in the channel. This approximation is accurate to leading order in the limit  $\varepsilon \rightarrow 0$  as long as two conditions are satisfied before the DDT onset: firstly, the flow stays of the same order as the initial laminar flame velocity  $u/a = O(\varepsilon)$ ; and, secondly, the flame acceleration does not involve time scales shorter than  $\tau_e$ . More details are given in § 3.2.
- (iii) In the initial formulation, exothermic reactions were neglected in the end-gas. This occurs if the induction delay is long enough compared with the time taken by the

combustion front to reach the closed end, as for example in runs 1 (neither detonation nor autoignition) and 5 (detonation onset) of Yu & Chen (2015) while autoignition develops ahead of the flame front in case 4. The assumption of an inert end-gas was relaxed by Kagan & Sivashinsky (2013), still using the low-Mach-number approximation and a one-step chemical reaction controlled by an Arrhenius law that are not suitable approximations for the detonation onset near autoignition.

### 3. Combustion in a closed channel for inert end-gas

Before addressing the drastic effect of chemical kinetics in the induction period, it is instructive to revisit the case of flames propagating in inert end-gas, essentially to present an analytical solution that will be useful in the following.

#### 3.1. One-dimensional non-dissipative flows

Equations of mass, momentum and energy in inert and non-dissipative planar flows yield

$$\frac{1}{\rho} \frac{D\rho}{Dt} = -\frac{\partial u}{\partial x}, \quad \frac{Du}{Dt} = -\frac{1}{\rho} \frac{\partial p}{\partial x}, \quad \rho c_p \frac{DT}{Dt} = \frac{Dp}{Dt}, \quad \text{where} \quad \frac{D}{Dt} \equiv \frac{\partial}{\partial t} + u \frac{\partial}{\partial x}. \quad (3.1)$$

For a perfect gas  $p = (c_p - c_v)\rho T$ ,  $(1/\rho)D\rho/Dt = (1/p)Dp/Dt - (1/T)DT/Dt$ , the energy equation in (3.1) takes the form of the entropy equation  $s(p, T)$ :

$$\text{entropy wave:} \quad \frac{Ds}{Dt} = 0 \Leftrightarrow \frac{1}{T} \frac{DT}{Dt} = \frac{\gamma - 1}{\gamma} \frac{1}{p} \frac{Dp}{Dt} \Leftrightarrow \frac{1}{\rho} \frac{D\rho}{Dt} = \frac{1}{\gamma} \frac{1}{p} \frac{Dp}{Dt}, \quad \text{where} \quad \gamma \equiv \frac{c_p}{c_v}. \quad (3.2)$$

Equations (3.1) can also be put in conservative form for the total energy  $e_{tot}$ :

$$\frac{\partial (\rho e_{tot})}{\partial t} = -\frac{\partial J}{\partial x}, \quad \text{where} \quad e_{tot} \equiv c_v T + u^2/2 + Q\psi \quad \text{and} \quad J \equiv \rho u \left( c_p T + u^2/2 + Q\psi \right) \quad (3.3)$$

with  $\psi = 1$  and  $\psi = 0$  in the unburned and burned gas, respectively,  $Q$  being the chemical energy liberated per unit mass by combustion.

#### 3.2. One-dimensional subsonic flows evolving slowly: low-Mach-number approximation

In a one-dimensional flow associated with a planar and markedly subsonic flame propagating in a closed tube, the momentum equation in (3.1) becomes non-useful as soon as the flame acceleration is small enough for making unimportant the drastic effect of the nonlinear compression waves pointed out long ago by the outstanding analysis of Riemann (1860), namely the formation of shock waves. This is not so obvious a mechanism that can be understood as a two-time-scale problem. The one-dimensional compressibility-induced disturbances (labelled by the subscript  $a$ ) are of the order of the Mach number (2.2)  $\delta u_a/\bar{u} = O(\varepsilon)$ ,  $\delta p_a/p \approx \delta u_a/a$  and oscillate on the short time scale of longitudinal acoustics in the tube,  $\tau_a \equiv L/a$ . The same effect is produced by weak shock waves bouncing back and forth by reflection on the walls delimiting the length of the closed tube. Focusing attention on a much longer time scale than  $\tau_a$ , the effect of these small oscillations vanishes by time averaging. Considering the mean flow  $(\bar{u}, \bar{p})$  evolving on the long time scale of the flame dynamics in a closed tube  $\tau_e/\tau_a = 1/\varepsilon$ , the relative difference along the tube of the time-averaged velocity and pressure is, respectively, of order unity and of second order  $\varepsilon^2$  (like across the flame), while the time evolution of both velocity and pressure is of order unity on the long time scale. For reasons that will become clear later, it is worth introducing a notation  $\dot{\tau}_e \equiv \bar{u}/(\partial \bar{u}/\partial t)$  different from the time scale of the

flame propagation in the tube ( $\dot{\tau}_e \leq \tau_e \approx L/U_L$ ):

$$\frac{\tau_a}{\dot{\tau}_e} = O(\varepsilon), \quad \frac{\dot{\tau}_e}{\bar{u}} \frac{\partial \bar{u}}{\partial t} = O(1) \quad \Rightarrow \quad \frac{L}{\bar{p}} \frac{\partial \bar{p}}{\partial x} = O(\varepsilon^2), \quad \frac{L}{\bar{u}} \frac{\partial \bar{u}}{\partial x} = O(1), \quad \frac{\dot{\tau}_e}{\bar{p}} \frac{\partial \bar{p}}{\partial t} = O(1). \quad (3.4)$$

Because of the nonlinear term  $u_a \partial u_a / \partial x$  (Reynolds stress), essential in the Riemann analysis, the time-averaging process is not straightforward. The assumption of a small flow acceleration  $1/\dot{\tau}_e \equiv (1/u)(\partial u/\partial t) \ll 1/\tau_a$  is a crucial issue for the validity of the low-Mach-number approximation (3.4) that can be broken down during the induction period of autoignition in the end-gas leading to the detonation onset studied in §§ 4 and 5. A rough dimensional analysis leading to (3.4) is worth recalling briefly, suppressing the overline and the subscript  $a$  for brevity of notation. According to the perfect gas law  $a^2/\gamma = p/\rho$ , the pressure gradient  $(1/\rho)(\partial p/\partial x)$  and the unsteady term  $\partial u/\partial t$  can be written, respectively, as  $(a^2/L)\delta p/p = (a/\tau_a)\delta p/p$  and  $\partial u/\partial t \approx \delta u/\dot{\tau}_e = (a/\dot{\tau}_e)(\delta u/a)$ . The balance of these two terms yields  $\delta p/p \approx (\tau_a/\dot{\tau}_e) \delta u/a$  recovering the relation of acoustic flows  $\dot{\tau}_e \approx \tau_a \Rightarrow \delta p/p \approx \delta u/a$ . If the mean flow varies on the long time scale  $\dot{\tau}_e \approx \tau_e \equiv (\tau_a/\varepsilon)$  and on the length scale  $L$ , the above balance shows that the relative variation of pressure along the tube is of order  $\varepsilon^2$  if the Mach number of the flow is small,  $u/a = O(\varepsilon) \Rightarrow \delta p/p = O(\varepsilon^2)$ . The same order of magnitude is obtained using the comparison with  $u \partial u/\partial x = O(\varepsilon^2 a^2/L)$ .

Before coming back to the one-dimensional case, it is worth recalling that the multi-dimensional problem is more involved because an additional length scale is introduced by the Darrieus–Landau instability, namely the intrinsic size of the cellular structure involving the laminar flame thickness to stabilise the short wavelength; see Clavin & Searby (2016) for an extensive presentation of the problem in free space.

To summarise, in a one-dimensional geometry and under the conditions (2.1)–(2.2), the flame can be treated as a discontinuity whose inner structure is in steady state. Under the additional condition (3.4) the pressure  $p(t)$  can be considered as uniform and the constitutive equations for the flow on both sides of the flame front reduce to the first and third equations in (3.1). These two equations for the temperature and the flow on each side of the flame front ( $T_u(x, t)$ ,  $u_u(x, t)$ ) and ( $T_b(x, t)$ ,  $u_b(x, t)$ ), the subscripts  $u$  and  $b$  denoting the unburned and burned gas, respectively, have to be solved with four boundary conditions, one at each tube end plus two others on the thin flame front involving the laminar flame velocity  $U_L$  (see (3.11) below). Knowing the function ‘laminar flame velocity versus the temperature just ahead of the flame front’  $U_L(T_{uf})$ , the solution for the flow leads to the time-dependent pressure  $p(t)$  and flame position  $X_f(t)$ . The problem is usually solved numerically. An analytical solution useful for the following is presented below.

### 3.3. Analytical solution of the simplified model presented in § 2

Introducing the unknown pressure growth rate  $1/\tau_p(t)$  and using the isentropic condition, the mass conservation reads

$$\frac{\partial u}{\partial x} = -\frac{1}{\tau_p(t)} < 0, \quad \text{where} \quad \frac{1}{\tau_p(t)} \equiv \frac{1}{\gamma} \frac{1}{p} \frac{dp}{dt} > 0. \quad (3.5)$$

The boundary conditions on the tube ends,  $u = 0$  for  $x = 0$  and  $x = L$ , yield

$$X_f(t) \leq x \leq L : u_u(x, t) = -\frac{(x-L)}{\tau_p(t)} > 0, \quad 0 \leq x \leq X_f(t) : u_b(x, t) = -\frac{x}{\tau_p(t)} < 0, \quad (3.6)$$

leading to the flow adjacent to the flame on both sides of the front in the form

$$\text{unburned gas side: } u_{uf}(t) \equiv u_u(x = X_f(t), t) = -\frac{[X_f(t) - L]}{\tau_p(t)} > 0, \quad (3.7)$$

$$\text{burned gas side: } u_{bf}(t) \equiv u_b(x = X_f(t), t) = -\frac{X_f(t)}{\tau_p(t)} < 0. \quad (3.8)$$

The linear distribution of flow speed in (3.6) was confirmed by the numerical simulations of Yang, Wang & Chen (2023) and Li *et al.* (2025).

In the absence of an entropy source in the end-gas, (3.2) shows that, the pressure being uniform, the thermodynamic state of the end-gas is also uniform,  $\rho_u(t)$ ,  $T_u(t)$ :

$$\text{end-gas: } \frac{p(t)}{p_0} = \left(\frac{\rho_u}{\rho_0}\right)^\gamma = \left(\frac{T_u}{T_0}\right)^{\gamma/(\gamma-1)}, \quad (3.9)$$

where the subscript 0 denotes the initial state of the unburned gas. Therefore, we have  $T_{uf} = T_u$ . In contrast, the thermodynamic state of the burned gas is not uniform because the burned gas side of the flame acts as an entropy source and the flame temperature increases with the flame position  $x = X_f(t)$ . This unsteady entropy is propagated by the flow towards the adiabatic wall at  $x = 0$  since  $u_b < 0$ , producing a gradient of temperature and density in the burned gas. This phenomenon, called ‘layered combustion’, was well explained by Zeldovich *et al.* (1985). It was observed a long ago in 1906 and described some time later. This question will not be addressed here. The flame dynamics  $X_f(t)$  is obtained from the solution of the end-gas flow, independently of the burnt-gas flow.

On the one hand, the flame position  $X_f(t)$  can be eliminated by subtracting (3.7) from (3.8):

$$u_{uf} - u_{bf} = \frac{L}{\tau_p(t)} = L \frac{1}{\gamma} \frac{1}{p} \frac{dp}{dt}. \quad (3.10)$$

On the other hand, the pressure drop across the flame being negligible (of order  $\varepsilon^2$ ), the jump  $u_{uf} - u_{bf}$  can be expressed in terms of the laminar flame velocity  $U_L$  and the chemical heat release per unit mass of unburned gas  $Q$ ,  $T_{bf} - T_u = Q/c_p$ , using the quasi-isobaric conservation of mass and energy across the flame structure in quasi-steady state:

$$U_f - u_{uf} = U_L, \quad U_f - u_{bf} = U_b = \frac{T_{bf}}{T_u} U_L \Rightarrow u_{uf} - u_{bf} = \left[ \frac{T_{bf}}{T_u} - 1 \right] U_L = \frac{Q}{c_p T_u} U_L, \quad (3.11)$$

where  $U_f(t) \equiv dX_f/dt$  denotes the propagation speed of the flame front in the reference frame of the tube,  $U_b = (T_{bf}/T_u)U_L$  being the laminar flame velocity relative to the burned gas. Putting together (3.10) and (3.11) yields the rate of pressure rise in terms of the laminar flame velocity:

$$\frac{L}{\tau_p(t)} = \frac{1}{\gamma} \frac{1}{p} \frac{dp}{dt} L = \frac{Q}{c_p T_u} U_L(T_u). \quad (3.12)$$

Then, the isentropic condition (3.9) in the end-gas leads to a closed equation for  $T_u(t)$ :

$$\frac{dT_u}{dt} = (\gamma - 1) \frac{Q}{c_p} \frac{U_L(T_u)}{L}. \quad (3.13)$$

Introducing the initial temperature  $T_0$ , the solution of (3.13) can be written

$$\int_1^{T_u/T_0} \frac{d(T_u'/T_0)}{U_L(T_u')/U_{L0}} = (\gamma - 1) \frac{Q}{c_p T_0} \frac{t}{\tau_e}, \quad \text{where } \tau_e \equiv \frac{L}{U_{L0}} \text{ and } U_{L0} \equiv U_L(T_0). \quad (3.14)$$

The reduced temperature  $T_u/T_0$  of the end-gas versus the reduced time  $t/\tau_e$  is obtained by inversion of (3.14). The integrant being positive, the solution can be obtained for any law  $U_L(T_u)$ , at least numerically. Once the function  $T_u(t)/T_0$  is known from (3.13)–(3.14), the pressure  $p(t)/p_0$  and the density of end-gas  $\rho_u(t)/\rho_0$  are given by the isentropic condition (3.9). The geometry occurring only through the divergence of the flow in (3.5), the solution is extended in a straightforward manner to cylindrical and spherical geometry.

The flame dynamics  $x = X_f(t)$  is directly obtained from  $p(t)$  and  $\rho_u(t)$  by the conservation of total energy (3.3) (see (3.17) below). In the limit of small Mach number, the term  $u^2/2$  introduces a negligible correction of order  $\varepsilon^2$  in the total energy  $e_{tot} \approx c_v T + Q\psi$  and in the flux  $J \approx [(\gamma - 1)/\gamma]up + \rho u Q$ . Integration of (3.3) for adiabatic walls,  $J_b|_{x=0} = J_u|_{x=L} = 0$ , yields in the burned and unburned gas, respectively,

$$\psi = 0, \quad \int_0^{X_f(t)} c_v \frac{\partial(\rho T)}{\partial t} dx = -J_b|_{x=X_f(t)} = -u_{bf}(t) \frac{\gamma}{\gamma - 1} p(t), \quad (3.15)$$

$$\psi = 1, \quad \int_{X_f(t)}^L \left[ c_v \frac{\partial(\rho T)}{\partial t} + Q \frac{\partial \rho_u}{\partial t} \right] dx = J_u|_{x=X_f(t)},$$

$$\text{where } J_u|_{x=X_f(t)} = u_{uf}(t) \left[ \frac{\gamma}{\gamma - 1} p(t) + Q \rho_{uf}(t) \right]. \quad (3.16)$$

Using the perfect gas law  $p \propto \rho T$  with the approximation of  $p(t)$  uniform in the tube, the continuity equation (3.1) written in conservative form  $\partial \rho_u / \partial t = -\partial(\rho_u u_u) / \partial x$  and the impermeable condition at the wall  $x = L : u_u = 0$ , (3.15) and (3.16) read  $X_f dp/dt = -\gamma u_{bf} p$  and  $(L - X_f) dp/dt = \gamma u_{uf} p$  that are the same as (3.7)–(3.8) leading to (3.10). The global form of the conservation of total energy was used by Zeldovich *et al.* (1985) to show that the pressure increases linearly with the mass fraction of burned gas (see (3.19) below). This is obtained in a straightforward manner by commuting the derivative with respect to the time and the integral in (3.15)–(3.16) that introduces the shift  $dX_f/dt$  in the flux. The inner structure of the flame being assumed in steady state, the fluxes relative to the flame front  $\rho[u - dX_f/dt]$  and  $[u - dX_f/dt][\gamma p/(\gamma - 1) + \rho q\psi]$  are the same on both sides of the moving flame. Therefore, the time derivative of the total energy flux obtained by adding these two equations is zero. Then, a uniform pressure  $p(t)$  in the channel and a uniform density in the end-gas  $\rho_u(t)$  yield

$$\frac{d}{dt} \left[ \int_0^{X_f(t)} c_v \rho_b T_b dx + \int_{X_f(t)}^L (c_v \rho_u T_u + Q \rho_u) dx \right] = 0 \Rightarrow p + (\gamma - 1) Q \left( 1 - \frac{X_f}{L} \right),$$

$$\rho_u = \text{const.}, \quad (\gamma - 1) Q \rho_u(t) X_f(t)/L = p(t) - p_0 + (\gamma - 1) Q [\rho_u(t) - \rho_0], \quad (3.17)$$

$$t = 0 : X_f = 0, \quad p = p_0; \quad X_f = L : p = p_e \equiv p_0 + (\gamma - 1) Q \rho_0 \quad (3.18)$$

leading to

$$\frac{p - p_0}{p_e - p_0} = 1 - \frac{\rho_u(t)[L - X_f(t)]}{\rho_0 L}. \quad (3.19)$$

This is the result of Zeldovich *et al.* (1985) indicating that the relative pressure rise is equal to the mass fraction of burned gas. When all the mixture is burned, i.e.  $X_f = L$ , the

pressure is equal to the equilibrium pressure,  $p = p_e$ . Note that the end-gas is assumed to be frozen since the exothermic reactions are neglected.

### 3.4. Finite-time singularity

Coming back to the closed equation for the temperature of the unburned gas in (3.14), the laminar flame velocity being a nonlinear function increasing with the unburned gas temperature  $T_u$ , the solution  $T_u(t)$  of (3.13)–(3.14) is singular after a finite time as soon as the thermal sensitivity of the laminar flame velocity  $U_L(T_u)$  is large enough. This can be illustrated by a power law  $U_L/U_{L0} = \theta^n$ , where  $\theta \equiv T_u/T_0$ , the general property of the solution depending on the sign of  $n - 1$ . Introducing the notation  $\tau \equiv (\gamma - 1)(Q/c_p T_0) (t/\tau_e)$  for the reduced time, the solution of (3.14) is

$$\begin{aligned} n > 1 : \theta &= \frac{1}{[1 - (n - 1)\tau]^{1/(n-1)}}; & n < 1 : \theta &= [1 + (1 - n)\tau]^{1/(1-n)}; \\ n = 1 : \theta &= \exp \tau, \end{aligned} \quad (3.20)$$

showing a finite-time singularity for  $n > 1$ . The larger is  $n - 1 > 0$ , the stronger is the singularity and the smaller the critical time  $t_c$ :

$$\tau_c = \frac{1}{n - 1} \Leftrightarrow t_c = \frac{\tau_e}{(n - 1)(\gamma - 1)Q/c_p T_0}, \quad \tau_e \equiv L/U_{L0} \equiv L/U_L(T_0). \quad (3.21)$$

A similar result is obtained with the exponential expression of the laminar flame velocity by the asymptotic theory of Zeldovich & Frank-Kamenetskii (1938) in the limit of large activation energy (the pre-factor being neglected):  $U_L(T_u)/U_L(T_0) = \exp[-(E/2k_B)(1/T_{bf} - 1/T_{b0})]$  with  $T_{b0} = T_0 + Q/c_p$  and  $T_{bf} = T_u + Q/c_p$ . Approximating  $\theta \equiv T_u/T_0 \approx 1$  in front of  $(Q/c_p T_0)$  for simplicity, we have

$$\begin{aligned} \frac{U_L(T_u)}{U_L(T_0)} &= \exp[b(\theta - 1)], & b &\equiv \frac{1}{2} \frac{E}{k_B T_{b0}} \frac{1}{(\theta + Q/c_p T_0)} \\ & & b &\approx \frac{1}{2} \frac{E}{k_B T_{b0}} \frac{1}{(1 + Q/c_p T_0)} > 0, \end{aligned} \quad (3.22)$$

in which  $b$  is approximated by a positive parameter of order unity. Substituting (3.22) into the integral on the left-hand side of (3.14) yields

$$\theta = 1 - \frac{\ln(1 - b\tau)}{b}, \quad \tau \equiv (\gamma - 1)(Q/c_p T_0) (t/\tau_e), \quad (3.23)$$

which shows a logarithmic singularity for the temperature of the end-gas at the critical time  $t_c$ :

$$\tau_c = \frac{1}{b} \Leftrightarrow t_c = \frac{\tau_e}{b(\gamma - 1)Q/c_p T_0}, \quad \tau_e \equiv L/U_{L0} \equiv L/U_L(T_0). \quad (3.24)$$

This singularity is physically relevant if and only if the critical time (3.21) or (3.24) is smaller than the transit time of the flame in the tube  $t_c < t_{end}$ ,  $\int_0^{t_{end}} U_f(t) dt = L$ . This cannot be the case with an inert end-gas since, according to (3.9) and (3.19),  $p$  and  $\rho_u$  are necessarily bounded for  $X_f/L \leq 1$  under the low-Mach-number approximation characterised by a uniform pressure  $p(t) \leq p_e$  (see (3.18)). The relation  $t_{end} < t_c$  is checked directly on the preceding example (3.22) from  $U_f > U_L \Rightarrow X_f/L > \int_0^t (U_L/L) dt' \Rightarrow 1 > \int_0^{t_{end}} \exp[b(\theta - 1)] dt/\tau_e$  to give  $(\gamma - 1)(Q/c_p T_0) > \int_0^{\tau_{end}} d\tau/[1 - b\tau]$ , in which (3.23) for the reduced variable  $\tau$  is used. Using  $\tau_c \equiv 1/b$ , we have  $b(\gamma - 1)(Q/c_p T_0) >$

$\int_0^{\tau_{end}/\tau_c} d(\tau/\tau_c)/[1 - (\tau/\tau_c)] \Rightarrow \tau_{end}/\tau_c < 1$ . To conclude, the singularity is not relevant for an inert end-gas. What about the end-gas during the induction period delay preceding autoignition? This problem is the topic of § 4.

#### 4. Transition to detonation just before autoignition of the end-gas

The purpose of this section is to explore the role of autoignition and more specially the key effect of the large thermal sensitivity of the induction period, a phenomenon that cannot be captured by a one-step kinetic model of combustion. This is enlightened by comparison with the one-step model investigated numerically by Kagan & Sivashinsky (2013) and revisited briefly now.

##### 4.1. Autoignition of the end-gas in the low-Mach-number regime

Still using the low-Mach-number formalism, Kagan & Sivashinsky (2013) added a uniform heat release rate to the energy equation (3.1) in the end-gas, controlled by the same one-step reaction scheme governing the flame, denoting  $\psi_u$  as the mass fraction of the limiting species,

$$\rho_u c_p \frac{dT_u}{dt} = \frac{dp}{dt} + \rho_u Q \frac{\psi_u}{\tau_r(T_u)}, \quad \frac{d\psi_u}{dt} = -\frac{\psi_u}{\tau_r(T_u)}, \quad t = 0: \psi_u = 1, \quad X_f = 0, \quad (4.1)$$

using the same mass and momentum equations as in (3.1).

From a mathematical point of view, particular attention should be paid to keep meaningful the inner structure of the flame treated as a peculiar kind of reaction–diffusion wave (see §§ 8.3–8.4 in Clavin & Searby (2016) for an extensive discussion of this question). The reaction rate in the unburned gas should be fully negligible compared with the reaction rate at the flame temperature  $1/\tau_{ru} \ll 1/\tau_{rb}$ , with  $\tau_{ru} \equiv \tau_r(T_u)$  and  $\tau_{rb} \equiv \tau_r(T_{bf}) \approx d_L/U_L$  denoting, respectively, the reaction time scales at the unburned gas temperature  $T_u$  and at the flame temperature  $T_{bf} = T_u + Q/c_p$ . It turns out that an extremely large difference of combustion time scales  $\tau_{ru} \gg \tau_{rb}$  can be handled for describing autoignition of the end-gas before the flame reaches the end of the channel at a time of the order  $\tau_e = L/U_L \approx (L/d_L)\tau_{rb}$ , using  $\tau_{rb} \approx d_L/U_L$ . It is sufficient to consider tubes long enough. A rough estimation involves considering  $\tau_{ru}$  as the induction time assumed constant for simplicity to give  $\tau_e/\tau_{ru} = O(1)$  yielding  $(L/d_L)(\tau_{rb}/\tau_{ru}) = O(1)$ . This leads to a realistic tube length for ordinary combustible mixtures governed by an Arrhenius law:

$$\frac{L}{d_L} \approx \exp \left[ \frac{E}{k_B T_b} \frac{Q}{c_p T_u} \right] \approx 10^3, \quad (4.2)$$

the numerical value  $10^3$  corresponding to  $E/k_B T_b \approx 3.5$  at  $T_u = 1000$  K and  $T_b = 3000$ , leading to  $L \approx 10$  cm. Introducing the solution of (4.1)  $\psi_u(t)$ , the conservation of total energy takes a similar form as before:

$$\begin{aligned} \frac{d}{dt} \left[ \int_0^{X_f(t)} c_v \rho_b T_b dx + \int_{X_f(t)}^L (c_v \rho_u T_u + Q \rho_u) \psi_u dx \right] &= 0 \\ \Rightarrow p(t) + (\gamma - 1) Q \left( 1 - \frac{X_f(t)}{L} \right) \psi_u(t) \rho_u(t) &= \text{const.}, \\ \frac{p(t) - p_0}{p_e - p_0} &= 1 - \frac{\rho_u(t) \psi_u(t) [L - X_f(t)]}{\rho_0 L}. \end{aligned} \quad (4.3)$$

Unfortunately, because of the heat release in the end-gas in (4.1), the isentropic condition is no longer valid and there is no analytical solution valid up to the end. However, the temperature of the end-gas can be computed analytically during a large part of the combustion process in the tube. More precisely, during most of the induction period, the mass fraction of reactants remains close to its initial value,  $\psi_u \approx 1$ . Then, (4.1) associated with (3.12) leads to a closed equation for  $T_u(t)$ :

$$\frac{dT_u}{dt} = \frac{Q}{c_p} \left[ (\gamma - 1) \frac{U_L(T_u)}{L} + \frac{1}{\tau_r(T_u)} \right], \quad (4.4)$$

which can be solved by quadrature in the same way as in (3.14) showing a singularity in finite time. But, as before, the runaway of temperature obtained from (4.4) cannot be observed before the end of the combustion process because the upper bound of pressure  $p_e$  is still imposed by the low-Mach-number approximation.

The problem (4.1) has been addressed numerically by Kagan & Sivashinsky (2013). When the combustion ends before the flame reaches the closed end of the channel on the unburned side, their numerical results show an abrupt homogeneous (volumetric) autoignition of the whole end-gas ahead of the flame. A sudden inversion of the flow  $u_u$  is shown by the numerics during the final sharp rise of pressure and temperature of the end-gas. In the words of the authors, this phenomenon is well beyond the range of the model's validity. As explained in the next subsection, the small-Mach-number approximation is no longer valid as soon as the flame acceleration becomes large enough under the joint effect of the small heat release at low temperature in the end-gas and the thermal sensitivity of the laminar flame velocity.

#### 4.2. Deflagration-to-detonation transition in the numerical simulations

The combustion dynamics reported in the preceding section, obtained with a one-step chemistry and a low-Mach-number approximation, has nothing to do with case 5 of the simulation results of Yu & Chen (2015) concerning flame propagation and DDT in a 2 cm channel filled with a hydrogen–air mixture at 10 atm and 1100 K. The temperature of the end-gas stays close to 1100 K (never larger than 1200 K) up to the end of the combustion process and the flame velocity stays about  $U_f \approx 70 \text{ cm s}^{-1}$  before a sharp transition in flame acceleration leading to the DDT occurring at about  $X_f \approx 0.6\text{--}0.8 \text{ cm}$ , the rest of the end-gas being burnt in a few microseconds by the propagation of the detonation before volumetric explosion by autoignition. The objective of this section is to explain the DDT mechanism for such an initial condition of a planar flame starting near an endwall with a low-Mach-number mode in a closed channel of relatively small length. The chemical kinetics controlling the induction delay below the ‘crossover temperature’ (as it is called in chemical kinetics of hydrogen–oxygen combustion) play an important role.

#### 4.3. Induction delay below the crossover temperature

The complex chemical kinetics of hydrogen–oxygen mixtures is well understood as a result of the theoretical analyses of Sánchez & Williams (2014), Sánchez *et al.* (2014) and Boivin *et al.* (2012). A detailed presentation of the systematically reduced kinetic scheme derived by those authors is beyond the scope of this article. The essential results for the conditions in the end-gas studied here (about 1150 K and 10 atm) are summarised as follows. The crossover temperature (1500 K at 10 atm) corresponds to a balance between the rate of production and consumption of hydrogen atoms by, respectively, the shuffle reactions (chain-branching) and the recombination of H with O<sub>2</sub> (chain-breaking) producing HO<sub>2</sub> (hydroperoxyl) that is recycled to produce H<sub>2</sub>O<sub>2</sub> (hydrogen peroxide).

The thermal sensitivity  $b$  of the flame propagation is governed by the shuffle reactions at the flame temperature ( $T_b \approx 3000$  K) to give a moderate flame sensitivity  $b$  between 2 and 3. The induction period of the homogeneous end-gas for temperature  $T_u$  between 1100 and 1200 K (well below crossover) is governed by a thermal explosion in which, the hydrogen atoms being maintained in extremely small concentration and the consumption of reactants negligible, the rate of heat release is governed by the hydrogen peroxide dissociation whose activation energy is very large (about 25 700 K) compared with that of the shuffle reactions (about 8590 K). The overall thermal sensitivity  $\beta_i$  of the resulting induction time at 1250 K is about 13, about 5 times larger than  $b$ . A key point of the DDT phenomenon is the time scale of this precursor phenomenon which is highly sensitive to temperature  $T_u$ , as illustrated by the variation of the induction delay  $\tau_{ind}$  with the temperature. In a stoichiometric hydrogen–air mixture at  $p = 10$  atm,  $\tau_{ind}$  decreases by a factor of about  $10^{-3}$ – $10^{-4}$  when  $T_u$  increases by a few hundred kelvins around 1000 K (see Sánchez & Williams 2014). To be more precise concerning case 5 investigated by Yu & Chen (2015), starting with an initial temperature  $T_u = 1100$  K for which the induction delay is about  $\tau_{ind} \approx 5 \times 10^{-4}$  s, the transition to detonation occurs at  $T_u \approx 1200$  K for which the induction delay is 50 times smaller,  $\tau_{ind} \approx 10^{-5}$  s. The numerical results presented in § 5 are based on the full chemical scheme controlling the  $H_2/O_2$  combustion. The drastic effect of the chemical kinetics below crossover is not easily assessed with a one-step kinetics scheme governed by a single Arrhenius law. Moreover, the use of detailed chemical kinetics in an analytical description of the detonation onset is beyond the scope of the present article.

#### 4.4. Ultra-simplified kinetic model

In this section, we develop a theoretical analysis based on a model considering a law of reaction rate of heat release different at the low temperature  $T_u \approx 1100$ – $1200$  K of the end-gas from that at the high temperature  $T_b = T_u + Q/c_p \approx 2500$ – $3000$  K controlling the flame propagation. Three assumptions are made: firstly, the reaction rate is much more sensitive to temperature at low temperature ( $T \approx T_u$ ) than at high temperature  $T_b$ ; secondly, the heat release per unit mass  $q$  during the induction process ( $T \approx T_u$ ) is much smaller than  $Q$  liberated by the full combustion; and thirdly, the consumption of reactants is negligible at low temperature ( $T \approx T_u$ ) during the induction period. In case 5 of the numerical simulation by Yu & Chen (2015), the chemical heat release per unit mass of reactive mixture  $q$  during the induction period (in the end-gas) is typically  $10^2$  to  $10^3$  times smaller than the total heat release by the complete combustion  $q/Q \approx 10^{-2}$ . Introducing the rate of heat release  $1/\tau_{ri}(T_u)$  during the induction period, whose thermal sensitivity  $\beta_i \equiv -(T_u/\tau_{ri})\partial\tau_{ri}/\partial T_u$  is as large as that of the induction delay  $\tau_{ind}$ ,  $\beta_i \tau_{ind}/(-T_u \partial\tau_{ind}/\partial T_u) = O(1)$ , and recalling that the consumption of reactants is negligible during the induction period, (4.1) in the end-gas is replaced by

$$\rho_u c_p \frac{dT_u}{dt} \approx \frac{dp}{dt} + \rho_u q \frac{1}{\tau_{ri}(T_u)} \Leftrightarrow \frac{1}{T_u} \frac{dT_u}{dt} \approx \frac{\gamma - 1}{\gamma} \frac{1}{p} \frac{dp}{dt} + \frac{q/(c_p T_u)}{\tau_{ri}(T_u)}, \quad \psi_u \approx 1, \quad (4.5)$$

to give, using (3.12), a closed equation for the temperature of the end-gas:

$$\frac{dT_u}{dt} \approx (\gamma - 1) \frac{Q/c_p}{\tau_e(T_u)} + \frac{q/c_p}{\tau_{ri}(T_u)}, \quad \tau_e(T_u) \equiv \frac{L}{U_L(T_u)} \approx 300 \mu\text{s}, \quad \tau_{ind}(T_u) \approx 100 \mu\text{s}, \quad (4.6)$$

characterising the low-Mach-number regime of flame propagation during the induction period. The first and second terms on the right-hand side of (4.6),  $(\gamma - 1)(Q/c_p)/\tau_e$

and  $(q/c_p)/\tau_{ri}$ , describe, respectively, the small temperature rise by low-Mach-number compression and induction kinetics below crossover.

The time scale  $\tau_e(T_0) = L/U_L(T_0)$  is a measure of the initial transit time of the flame across the channel in the absence of DDT or autoignition. It is much larger than the acoustic time  $\tau_e \gg \tau_a = L/a$ ,  $\tau_e/\tau_a = 1/\varepsilon$ . For  $T_0 \approx 1100$  K and  $p_0 \approx 10$  atm, both time scales  $\tau_e$  and  $\tau_{ind}$  are initially of the same order of magnitude, but  $\tau_{ind}(T_u)$  decreases with the temperature  $T_u$  faster than  $\tau_e(T_u)$  and becomes quickly smaller than  $\tau_e$ . Autoignition develops immediately after the induction delay  $\tau_{ind}$ , while the flame has propagated on a distance typically larger than one third of the channel length  $\tau_{ind} \gtrsim \tau_e/3$ .

The full dynamics is characterised by four time scales:  $\tau_L \approx \tau_{rb} \equiv \tau_r(T_b)$ ,  $\tau_a = L/a$ ,  $\tau_e \equiv L/U_L$  and  $\tau_{ri}(T_u)$  with  $\tau_{ri}/\tau_{ind} = O(1)$ . The transit time of a fluid particle across the quasi-isobaric flame  $\tau_L \equiv d_L/U_L \lesssim 5 \mu\text{s}$  is not much larger than the reaction time at the flame temperature  $\tau_{rb} \approx 1 \mu\text{s}$ , but  $\tau_L$  is markedly smaller than the acoustic time  $\tau_a = L/a \approx 20 \mu\text{s}$  that is itself smaller than the transit time of the flame across the channel (in the absence of autoignition)  $\tau_e \equiv L/U_L \approx 300 \mu\text{s}$  ( $U_f \approx U_L$ ). In terms of the Mach number  $\varepsilon \equiv U_L/a$ , one has the relations  $\tau_L/\tau_a \approx (d_L/L)/\varepsilon \approx 10^{-1}$  and  $\tau_a/\tau_e = \varepsilon$ . To summarise, the following relations between the time scales hold during all the combustion process:  $\tau_{rb} \lesssim \tau_L \ll \tau_a \ll \tau_e$ . Moreover, at the initial condition one has  $\tau_{ind}/\tau_e = O(1)$ :

$$\text{initial condition, } t = 0, T = T_0: \quad \tau_L \ll \tau_a \ll \tau_e \approx \tau_{ind}, \quad \tau_{ri}/\tau_{ind} = O(1). \quad (4.7)$$

During most of the induction period, as long as the time scale characterising the induction-induced heating of the end-gas is larger than the time scale controlling the inner flame structure  $\tau_L \ll \tau_{ind}$ , the flame structure is described by the Zeldovich–Frank-Kamenetskii analysis (Zeldovich & Frank-Kamenetskii 1938) and is still controlled by the rate of heat release at high temperature  $1/\tau_{rb}$ . Introducing the combustion time scale at high temperature  $\tau_{rb} \equiv \tau_r(T_b) \approx d_L/U_L(T_u)$  into the the first term on the right-hand side of (4.6) and using  $\tau_e \equiv L/U_L$ , we get

$$\frac{dT_u}{dt} \approx (\gamma - 1) \frac{d_L}{L} \frac{Q/c_p}{\tau_r(T_b)} + \frac{q/c_p}{\tau_{ri}(T_u)}, \quad (4.8)$$

illustrating how small is the initial heating rate of the end-gas by both adiabatic compression and induction reactions compared with the exothermic reaction rate at high temperature inside the flame structure  $(Q/c_p T_u)/\tau_r(T_b)$ . The very small factor  $d_L/L$  in front of  $(Q/c_p T_u)/\tau_r(T_b)$  makes the heating rate by adiabatic compression sufficiently small to keep meaningful the inner structure of the flame evolving in a quasi-steady-state approximation. A very small increase in temperature makes the reaction rate  $1/\tau_{ri}$  increase considerably so that  $\tau_{ri}$  becomes quickly of same order of magnitude as the acoustic time. However, the end-gas is warmed up at a rate still smaller than at high temperature inside the flame structure  $(Q/c_p T_b)/\tau_{rb}$ . But  $(q/c_p)/\tau_{ri}$  becomes quickly larger than the heating rate by the low-Mach-number compression, namely the first term on the right-hand side (4.8) proportional to  $d_L/L \ll 1$ . After the delay  $t_I$  making the second term on the right-hand side of (4.8) larger than the first term, (4.8) reduces to

$$t > t_I: \quad \frac{dT_u}{dt} \approx \frac{q/c_p}{\tau_{ri}(T_u)}. \quad (4.9)$$

This delay  $t_I$  corresponds roughly to the time at which the heating rate of the end-gas by the reactions controlling the induction delay below the crossover temperature becomes of the same order of magnitude as the adiabatic compression during the small-Mach-number propagation of the flame. According to (4.6), this occurs at a temperature  $T_{ui}$  defined by

$$t = t_I : T_u = T_{ui}, \quad \frac{q/c_p}{\tau_{ri}(T_{ui})} = (\gamma - 1) \frac{Q/c_p}{\tau_e(T_{ui})}, \quad \text{where} \quad \frac{1}{\tau_e(T_{ui})} \equiv \frac{U_L(T_{ui})}{L}. \quad (4.10)$$

The reaction time  $\tau_{ri}(T_u)$  decreasing quickly when the temperature  $T_u$  increases, the reaction rate  $1/\tau_{ri}$  is a strongly increasing function of  $T_u$  so that, as explained in § 3.4, (4.9) exhibits a finite-time runaway of the end-gas temperature  $T_u(t)$  denoting a transition in the rate of heat release by the volumetric autoignition of the end-gas, as explained below (4.12). To show that the temperature runaway given by (4.9) occurs inside the channel as soon as the thermal sensitivity  $\beta_i$  of the reaction rate  $1/\tau_{ri}(T_u)$  is large enough, consider for simplicity a reaction rate  $1/\tau_{ri}(T_u)$  governed by an Arrhenius law  $1/\tau_{ri}(T_u) \approx \exp[\beta_i(\theta_i - 1)]/\tau_{ri}(T_{ui})$ , the reduced temperature  $\theta_i \equiv T_u/T_{ui}$  being scaled by the temperature  $T_{ui}$  in (4.10),  $t = t_I : \theta_i = 1$ . The solution of (4.9) reads

$$1 - e^{-\beta_i(\theta_i - 1)} = \frac{t - t_I}{\Delta t_c} \Leftrightarrow \beta_i(\theta_i - 1) = -\ln \left[ 1 - \frac{(t - t_I)}{\Delta t_c} \right], \quad \frac{(t - t_I)}{\Delta t_c} \leq 1, \quad (4.11)$$

$$\text{where} \quad \frac{1}{\Delta t_c} \equiv \beta_i \frac{q}{c_p T_{ui}} \frac{1}{\tau_{ri}(T_{ui})} = \beta_i (\gamma - 1) \frac{Q}{c_p T_{ui}} \frac{U_L(T_{ui})}{L}. \quad (4.12)$$

According to (4.11),  $\lim_{\beta_i(\theta_i - 1) \rightarrow \infty} (t - t_I)/\Delta t_c = 1 \Leftrightarrow \lim_{t \rightarrow t_I + \Delta t_c} \beta_i(\theta_i - 1) = \infty$  so that, in the limit  $\beta_i \gg 1$ , the singularity concerns a small reduced temperature  $(T_u - T_{ui})/T_{ui} = O(1/\beta_i)$ . According to (4.12), the delay  $\Delta t_c$  is of the same order of magnitude as the reaction rate  $\tau_{ri}(T_{ui})$  if  $\beta_i q/c_p T_{ui} = O(1)$  in the double limit  $\beta_i \gg 1$  and  $q/(c_p T_{ui}) \ll 1$ . The distance travelled by the flame between  $t = t_I$  and the critical time  $t_I + \Delta t_c$  is obtained by integration on the time  $\Delta X_f \approx \int_{t_I}^{t_I + \Delta t_c} U_L(T_u) dt = U_L(T_{ui}) \int_{t_I}^{t_I + \Delta t_c} \exp[b(\theta_i - 1)] dt$  with (4.11)–(4.12):

$$\frac{U_L(T_u)}{U_L(T_{ui})} = e^{b(\theta_i - 1)} = \frac{1}{[1 - (t - t_I)/\Delta t_c]^{b/\beta_i}} \quad (4.13)$$

$$\Rightarrow \Delta X_f = \frac{U_L(T_{ui}) \Delta t_c}{1 - b/\beta_i} \approx U_L(T_{ui}) \Delta t_c = \frac{L/[\beta_i(\gamma - 1)]}{Q/(c_p T_{ui})}. \quad (4.14)$$

The ratio  $b/\beta_i \ll 1$  been neglected in (4.14). Neglecting the rate of chemical heat release before  $t_I$ , the solution is the same as in § 3.3, with a rate of temperature increase (3.13) proportional to  $1/\tau_e(T_u)$  times a factor of order unity  $(\gamma - 1)(Q/c_p T_u) \approx 2$  so that the temperature  $T_{ui}$  can easily be reached after a distance travelled by the flame of a fraction of  $L$ . Therefore, because of the kinetics-induced temperature runaway (4.11)–(4.14), the total distance travelled by the flame during the induction delay  $\tau_{ind}(T_0) \equiv t_I + \Delta t_c$  can easily be smaller than the tube length  $L$ . The larger the thermal sensitivity of the chemical kinetic scheme controlling the chain-branching reactions  $\beta_i(\gamma - 1)Q/c_p T_{ui} \gg 1$ , the closer to  $t_I$  is the singularity of  $\beta_i(\theta_i - 1)$  in (4.11).

According to (4.13), the flame acceleration increases when approaching the induction delay:

$$\frac{1}{U_L(T_u)} \frac{\partial U_L}{\partial t} = \frac{b}{\beta_i} \frac{1}{\Delta t_c} \frac{1}{[1 - (t - t_I)/\Delta t_c]^{1+b/\beta_i}} \approx \frac{b}{\beta_i} \frac{1}{t_I + \Delta t_c - t}, \quad (4.15)$$

the last approximation being valid in the limit  $b/\beta_i \ll 1$ . The inner structure of the laminar flame is in quasi-steady state and is close to the solution of Zeldovich & Frank-Kamenetskii (1938) as long as the acceleration time scale  $\dot{\tau}_e$  is larger than the transit time

across the flame structure  $\tau_L$ :

$$\tau_L < \dot{\tau}_e \equiv \frac{U_L}{\partial U_L / \partial t} = \frac{\beta_i}{b} (t_I + \Delta t_c - t) \Leftrightarrow (t_I + \Delta t_c - t) > \frac{b}{\beta_i} \tau_L. \quad (4.16)$$

The flame acting as a self-accelerating semi-transparent piston, the low-Mach-number approximation of the end-gas flow breaks down when  $\dot{\tau}_e$  becomes smaller than  $\tau_a/\varepsilon$ , according to § 3.2. Equation (4.15) then puts the condition of breakdown of the low-Mach-number approximation in the form

$$(t_I + \Delta t_c - t) < \frac{b}{\beta_i} \frac{\tau_a}{\varepsilon}, \quad b/\beta_i = O(\varepsilon) \Rightarrow (t_I + \Delta t_c - t) < \tau_a. \quad (4.17)$$

Therefore, according to (4.16) and (4.17), assuming  $\tau_L < \tau_a/\varepsilon$ , the low-Mach-number approximation breaks down when the structure of the inner flame is in quasi-steady state:

$$\frac{b}{\beta_i} \tau_L < (t_I + \Delta t_c - t) < \frac{b}{\beta_i} \frac{\tau_a}{\varepsilon} \approx \tau_a. \quad (4.18)$$

#### 4.5. The DDT mechanism

The flame acceleration and the flow acceleration run away simultaneously in a finite time. Acceleration-induced compression waves propagating downstream (towards the closed end on the unburned gas side at  $x = L$ ) are launched from the maximum of flow velocity, namely from the leading edge of the flame. The compression waves become stronger and stronger as the flame acceleration increases, namely as the critical time  $t_I + \Delta t_c$  is approached. According to the nonlinear Riemann mechanism (Riemann 1860), shock waves are formed just ahead of the flame front. Then, in a way similar to the previous theoretical analyses of DDT (Clavin 2022, 2023, 2025) (but in a context different from the knocking studied here), the flame structure is blown off just before  $t \approx t_I + \Delta t_c$  by a thermal feedback loop between the shock and the flame, leading to a quasi-spontaneous formation of a detonation. According to the numerical simulation, the transition takes about  $1 \mu\text{s}$ . Propagating at about  $2000 \text{ m s}^{-1}$ , the detonation burns the last 1.2 cm of end-gas in less than  $6 \mu\text{s}$ , namely faster than the induction time  $\approx 100 \mu\text{s}$  at  $T_u = 1150 \text{ K}$  and  $p = 10 \text{ atm}$ . A key point is that, according to (4.16)–(4.18), the reaction–diffusion nature of the inner structure of the flame remains valid during the induction up to the transition, viewed as a catastrophic event for the inner structure of the laminar flame. A detailed analytical study of the short transient phenomena during which the inner structure of the flame is blown off is beyond the scope of the present article.

A problem worth investigating in the future is to decipher the DDT mechanism developing in some particular conditions on the closed end opposite to the flame ignition. It could be related to a thermal gradient built by cumulative nonlinear effects associated with the longitudinal acoustic waves in a closed channel since the pressure and temperature fluctuations are maximum on the closed ends.

## 5. Numerical simulation with a modified induction mechanism

To assess the effects of the chemical kinetics controlling the end-gas autoignition on the transition to detonation below the crossover temperature, the numerical simulations of case 5 conducted previously by Yu & Chen (2015) are reconsidered by modifying the reaction scheme that controls the induction period without influencing the inner structure of the laminar flame. The flame propagation and its transition to detonation are simulated using the same in-house code A-SURF as in Yu & Chen (2015). The numerical methods and settings are the same as those in Yu & Chen (2015) and thereby are not repeated here.

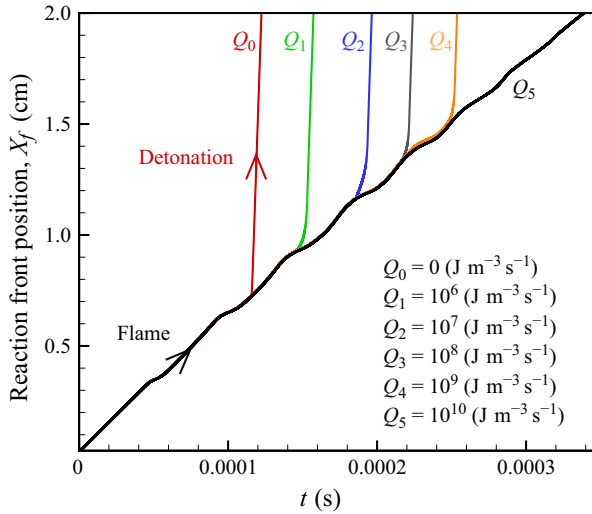


Figure 1. Evolution of the reaction front position.

Figure 1 shows the reaction front position as a function of time for different modifications of the reaction rates in the end-gas. The local flow is assumed to be frozen (i.e. to neglect all the elementary chemical reactions in the simulation) when the local heat release rate is below a threshold value  $Q_i$  ( $i = 0, 1, 2, 3, 4, 5$ ); otherwise the mixture is reactive and all chemical reactions are considered in the simulation. The thresholds  $Q_i$  are systematically much smaller than the maximum of heat release rate inside the inner structure of the laminar flame,  $Q_{max} \approx 10^{13} \text{ J m}^{-3} \text{ s}^{-1}$ . Before the sharp transition to detonation, the inner flame structure (and in particular the laminar flame velocity  $U_L$ ) is found to be insensitive to such small modifications that concern the heat release rate in a small range of end-gas temperature,  $\delta T_u / T_u$ , of a few per cent. For  $Q_0 = 0$ , all chemical reactions in the end-gas are considered as in Yu & Chen (2015) showing a transition to detonation 0.12 ms after flame ignition near the closed wall. When the threshold value increases to  $Q_1 = 10^6 \text{ J m}^{-3} \text{ s}^{-1} \approx 10^{-7} Q_{max}$  the transition to detonation is still observed but is delayed to 0.15 ms. For the largest value  $Q_5 = 10^{10} \text{ J m}^{-3} \text{ s}^{-1} \approx 10^{-3} Q_{max}$  that corresponds to the rate of heat release in the end-gas just before the transition to detonation when no modification of the chemical network is introduced, the end-gas is burned by the rightward-propagating flame and there is no transition to detonation. This confirms that the detonation mechanism is associated with the highly thermally sensitive rate of the small heat release during the induction period of the end-gas, as discussed in § 4.

## 6. Concluding remarks

The DDT mechanism of a one-dimensional flame initiated by a hot slide (planar hot pocket of burned gas) near the wall of a closed channel filled with a stoichiometric hydrogen–air mixture at  $p = 10 \text{ atm}$  and  $T = 1100 \text{ K}$  is different from that of the transition at the tip of an elongated flame initiated by a spark at the centre of a closed wall and propagating into a mixture at normal conditions of temperature and pressure. In the latter case, the transition to detonation occurs in a cold mixture (no autoignition) after a few milliseconds and the tube is long enough (about 2 m) for the compression waves generated by the self-accelerating flame and reflected by the opposite closed end to have not enough time to be back to the flame front before the detonation transition. The case considered here is

different. It concerns an initial mixture close to autoignition in a short tube (2 cm) and prompt to detonate. The initial condition is also quite different; the pressure is quasi-uniform in the closed vessel during the early stage of the flame propagation, the acoustic time being much shorter than the evolution time scale of the thermodynamic state of the unburned gas. The difference in the nature of the initial state is also worth stressing: stable initial composition at normal temperature ( $T = 300$  K) in the case of an elongated flame in a long tube while the initial state of the end-gas considered here to represent the knocking in internal combustion engines is close to autoignition with an induction delay decreasing quickly with a small increase in temperature during the induction process. In both cases, the transition to detonation is of a one-dimensional nature and is due to the ultimate compression waves generated during the last stage of strong flame acceleration. But, the origin of this ultimate acceleration is quite different: the back flow impinging on an elongated flame while it is the transient state of induction in the end-gas considered here. The key mechanism is here the large thermal sensitivity of the reactions controlling the induction delay below the crossover temperature, coupled with the increase in temperature associated with the flame propagation in a closed tube (before the detonation onset or the quasi-homogeneous autoignition of the end-gas). The rapid decrease of the time scale  $\tau_{ri}$  controlling the small heat release during the induction delay is essential for the DDT onset before the end of the induction period of the end-gas. During the short-lived transient stage (4.18) when the time scale  $\tau_{ri}$  becomes smaller than the acoustic time but larger than the transit time of a fluid particle across the flame structure, the reaction–diffusion nature of the flame remains meaningful. This short transient period of a strongly self-accelerated flame (acting as a semi-transparent piston) ends up with a catastrophic event blowing up the flame structure and leading to a spontaneous transition to detonation for no more than a microsecond. As on the tip of an elongated flame, it is the nonlinear thermal feedback loop (of thermal origin) between the laminar flame velocity and the acceleration-induced compression waves that is responsible for this catastrophic event. After the detonation onset, the rest of the end-gas is burned up faster by the detonation than it would be by the flame and/or the quasi-homogeneous autoignition of the end-gas.

**Acknowledgements.** Fruitful discussions with Dr Y. Morii at Manchester and Beijing are gratefully acknowledged. One of us (P.C.) thanks Professor C.K. Law for giving him the opportunity to interact with a very motivated audience and also with excellent groups of scientists during the summer schools of Princeton and Tsinghua.

**Funding.** The work at Peking University was supported by the National Natural Science Foundation of China (no. 52425604).

**Declaration of interests.** The authors declare that they have no known competing financial interests or personal relationships that could have appeared to influence the work reported in this paper.

#### REFERENCES

- BOIVIN, P., SÁNCHEZ, A.L. & WILLIAMS, F.A. 2012 Explicit analytic prediction for hydrogen–oxygen ignition times at temperatures below crossover. *Combust. Flame* **159**, 748–752.
- CICCARELLIA, G. & DOROFEEV, S. 2008 Flame acceleration and transition to detonation in ducts. *Prog. Energy Combust. Sci.* **34**, 499–550.
- CLAVIN, P. 2022 Finite-time singularity associated with the deflagration to detonation transition on the tip of an elongated flame-front in a tube. *Combust. Flame* **245**, 112347.
- CLAVIN, P. 2023 One-dimensional mechanism of gaseous deflagration-to-detonation transition. *J. Fluid Mech.* **974**, A6.
- CLAVIN, P. 2025 Physics of the transition to detonation of gaseous flames. *Europhys. Phys. J. Plus* **140**, 258.
- CLAVIN, P., PELCÉ, P. & HE, L. 1990 One-dimensional vibratory instability of planar flames propagating in tubes. *J. Fluid Mech.* **216**, 299–322.
- CLAVIN, P. & SEARBY, G. 2016 *Combustion Waves and Fronts in Flows*. Cambridge University Press.

- KAGAN, L. & SIVASHINSKY, G. 2013 Hydrodynamic aspect of end-gas autoignition. *Proc. Combust. Inst.* **34**, 857–863.
- LI, B.W., OTON-MARTINEZ, R.A., VELASCO, F.J.S., SÁNCHEZ, A.L. & WILLIAMS, F.A. 2025 Planar, cylindrical and spherical flame propagation in closed vessels with nonuniform composition and temperature. *Combust. Flame* **280**, 114379.
- LIBERMAN, M.A., IVANOV, M.F., KIVERIN, A.D., KUZNETSOV, M.S., CHUKALOVSKY, A.A. & RAKHIMOVA, T.V. 2010 Deflagration-to-detonation transition in high reactive combustible mixtures. *Acta Astronaut.* **67**, 688–701.
- MORII, Y., DUBEY, A.K., NAKAMURA, H. & MARUTA, K. 2021 Two-dimensional laboratory-scale DNS for knocking experiment using n-heptane at engine-like condition. *Combust. Flame* **223**, 330–336.
- RIEMANN, B. 1860 On the propagation of plane waves of finite amplitude (English translation 1980). *Intl J. Fusion Energy* **2**, 1–23.
- SIVASHINSKY, G.I. 1974 On propagation of flame in a closed vessel. *Israel J. Technol.* **12**, 317–321.
- SIVASHINSKY, G.I. 1979 Hydrodynamic theory of flame propagation in an enclosed volume. *Acta Astronaut.* **6**, 631–645.
- SÁNCHEZ, A.L., FERNÁNDEZ-TARRAZO, E. & WILLIAMS, F.A. 2014 The chemistry involved in the third explosion limit in H<sub>2</sub>-O<sub>2</sub> mixtures. *Combust. Flame* **161**, 111–117.
- SÁNCHEZ, A.L. & WILLIAMS, F.A. 2014 Recent advances in understanding of flammability characteristics of hydrogen. *Prog. Energy Combust. Sci.* **41**, 1–55.
- WANG, Z., HU, H. & REITZ, R.D. 2017 Knocking combustion in spark-ignition engines. *Prog. Energy Combust. Sci.* **61**, 78–112.
- WEI, H., ZHANG, X., ZENG, H., DEITERDING, R., PAN, J. & ZHOU, L. 2019 Mechanism of end-gas autoignition induced by flame-pressure interactions in confined space. *Phys. Fluids* **31**, 076106.
- YANG, L., WANG, Y. & CHEN, Z. 2023 Comparison of combustion duration and end-gas autoignition in inwardly and outwardly propagating flames induced by different ignition configurations. *Combust. Theory Model.* **27**, 103–117.
- YANG, L., WANG, Y., DAI, P. & CHEN, Z. 2024 Effect of temperature disturbance on end-gas autoignition and detonation development. *Proc. Combust. Inst.* **40**, 105220.
- YU, H. & CHEN, Z. 2015 End-gas autoignition and detonation development in a closed chamber. *Combust. Flame* **162**, 4102–4111.
- ZELDOVICH, YA B., BARENBLATT, G.I., LIBROVICH, V.B. & MAKHVILADZE, G.M. 1985 *The Mathematical Theory of Combustion and Explosions*. Consultants Bureau.
- ZELDOVICH, Y B. & FRANK-KAMEZNETSKII, D.A. 1938 A theory of thermal flame propagation. *Acta Phys. Chim.* **9**, 341–350.